FIRBACK Source Counts and Cosmological Implications

H. Dole[1], R. Gispert[1], G. Lagache[1], J-L. Puget[1], H. Aussel[2,3], F.R. Bouchet[4], P. Ciliegi[5], D.L. Clements[6], C.J. Cesarsky[7], F.X. Désert[8], D. Elbaz[2], A. Franceschini[3], B. Guiderdoni[4], M. Harwit[9], R. Laureijs[10], D. Lemke[11], R. McMahon[12], A.F.M. Moorwood[7], S. Oliver[13], W.T. Reach[14], M. Rowan-Robinson[13], and M. Stickel[11]

[1] Institut d'Astrophysique Spatiale, Orsay, France
[2] Service d'Astrophysique, CEA/DSM/DAPNIA Saclay, France
[3] Osservatorio Astronomico di Padova, Italy
[4] Institut d'Astrophysique de Paris, France
[5] Osservatorio Astronomico di Bologna, Italy
[6] Cardiff University, UK
[7] ESO, Garching, Germany
[8] Laboratoire d'Astrophysique, Observatoire de Grenoble, France
[9] 511 H.Street S.W., Washington, DC 20024-2725
[10] ISOC ESA, VILSPA, Madrid, Spain
[11] MPIA, Heidelberg, Germany
[12] Institute for Astronomy, University of Cambridge, UK
[13] Imperial College, London, UK
[14] IPAC, Pasadena, CA, USA

Abstract. FIRBACK is a one of the deepest surveys performed at 170 μm with ISOPHOT onboard ISO, and is aimed at the study of cosmic far infrared background sources. About 300 galaxies are detected in an area of four square degrees, and source counts present a strong slope of 2.2 on an integral "logN-logS" plot, which cannot be due to cosmological evolution if no K-correction is present. The resolved sources account for less than 10% of the Cosmic Infrared Background at 170 μm. In order to understand the nature of the sources contributing to the CIB, and to explain deep source counts at other wavelengths, we have developed a phenomenological model, which constrains in a simple way the luminosity function evolution with redshift, and fits all the existing deep source counts from the mid-infrared to the submillimetre range.

1 Introduction

The Cosmic Infrared Background (CIB), due to the accumulation of galaxy emission at all redshifts along the line of sight in an instrument beam, is a powerful tool for studying galaxy evolution. FIRBACK ([19], [5]), one of the deepest surveys performed at 170 μm, is aimed at the study of the CIB, in two complementary ways:

- study the resolved sources (this paper)
- study the background fluctuations ([13], [14])

Throughout this paper we use a cosmology with $h = 0.65$, $\Omega = 1$ and $\Lambda = 0$.

2 The FIRBACK Survey

FIRBACK, is a survey of 4 square degrees in 3 high galactic latitude fields, chosen to have as low an HI column-density as possible, typically $N_H \simeq 10^{20} cm^{-2}$, and if possible multiwavelength coverage. Observations were carried with ESA's Infrared Space Observatory (ISO, [12]) with the ISOPHOT photometer [16] in raster mode (AOT P22) with the `C200` camera and `C_160` broadband filter centered at $\lambda = 170\,\mu m$. A detailed description of the reduction, data processing, and calibration will be discussed in [15], whereas the analysis of the complete survey will be discussed in [6].

3 Source Counts at 170 μm

Preliminary FIRBACK integral source counts at $170\,\mu m$ (Fig. 1), not corrected for incompleteness, show a strong slope of 2.2 between 120 and 500 mJy. This strong slope is not explained by a K-correction or cosmological evolution alone: both must be present; the K-correction is the ratio, at a given wavelength, of the emitted flux over the redshifted flux.
Non (or low) evolution scenarii, or extrapolation of IRAS counts, are not able to reproduce the observed counts. For illustration, we plot in Fig. 1 the non-evolution model from [9] and the evolution model A from [11]. On the other hand, evolutionary models from [9] and from [11] (model E: evolution + ULIRGs) give a better agreement. At this wavelength, FIRBACK sources account for only 3% of the background.

4 Modelling the Evolution of Galaxies

4.1 Method

Our philosophy is to make a phenomenological model that explains all the observed deep source counts and reproduces the CIB in the mid-IR to submillimetre range. One way to do this is to constrain the evolution with redshift of the luminosity function (LF) in the infrared, given:

- templates of galaxy spectra
- the energy density available at each redshift

For the first point, we used template galaxy spectra based on IRAS colors [18] modified to account for recent ISO observations, in particular the absorption feature near $10\,\mu m$ at high luminosity; PAH features are present in the mid-infrared [4], even if their strength seems larger than the observations: this is not a problem because the right amount of energy is present in each peak, and we convolve the spectrum with the filter spectral response (Fig. 2). For the second point, we used the inversion of the CIB spectrum by [10] and [20], which gives with good accuracy the energy density available at redshifts between 1 and 3. This energy density is the integral of the luminosity function at each redshift, but there is no unique solution for the LF shape.

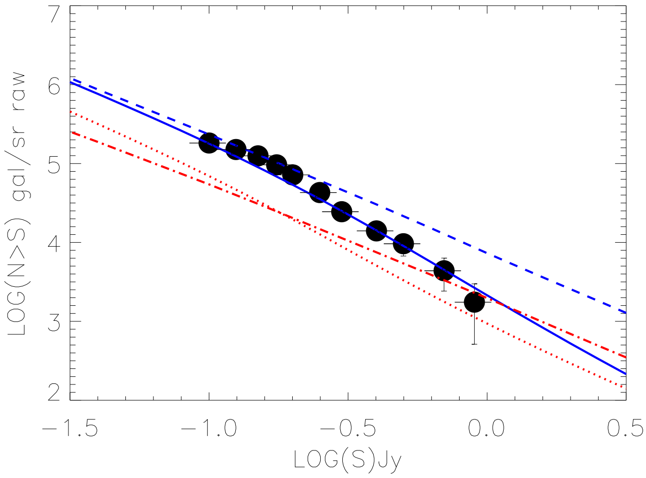

Fig. 1. FIRBACK integral source counts at 170 μm not corrected for incompleteness. Models from [11]: A (dot) with evolution, E (solid) with evolution + ULIRGs. Models from [9]: without evolution (dot-dash), with evolution (dash).

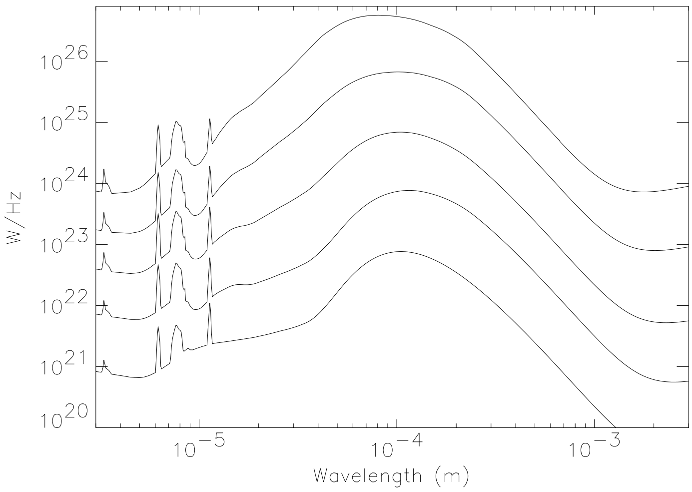

Fig. 2. Template spectra used for simulating source counts; from bottom to top: $L = 10^9$, 10^{10}, 10^{11}, 10^{12}, 10^{13} $L_\odot$.

4.2 Evolving Luminosity Function

The question is: how to evolve the LF with redshift ?
Fig. 3 represents the LF of [21] at a redshift z=0, renormalized to $h = 0.65$ and having the same integral as [23]. Our constraint on the LF redshift variation is the energy density available at each redshift [10]. Usually, authors apply a pure density evolution to the LF as a function of redshift (i.e. a vertical shift), or a pure luminosity evolution (a horizontal shift). This does not work for FIRBACK source counts: There is no alternative other than adding the evolution to one part of the LF only. This part is constrained by IR and submm observations: this is the bright end of the LF. Fig. 3 represents our decomposition of the local LF into two parts:

- left part: "normal" galaxies
- right part: ULIRG's, centered on a luminosity $L_{ULIRG} \simeq 2.0 \times 10^{11} L_{\odot}$, where L_{ULIRG} is the free parameter; we get the same value as [24]

In our model, "without evolution" means that the local LF (Fig. 3a) is taken, and is the same at every redshift. In the evolutionary scenario, only the ULIRG part moves, in such a way that the integral of the LF equals the constraint given by the CIB inversion at each redshift. The maximum is reached at $z \simeq 2.5$, and Fig. 3b represents the LF at this redshift. We neglect at this stage the evolution of "normal" galaxies, which do not play a crucial role in the mid-infrared to submillimetre wavelength range.

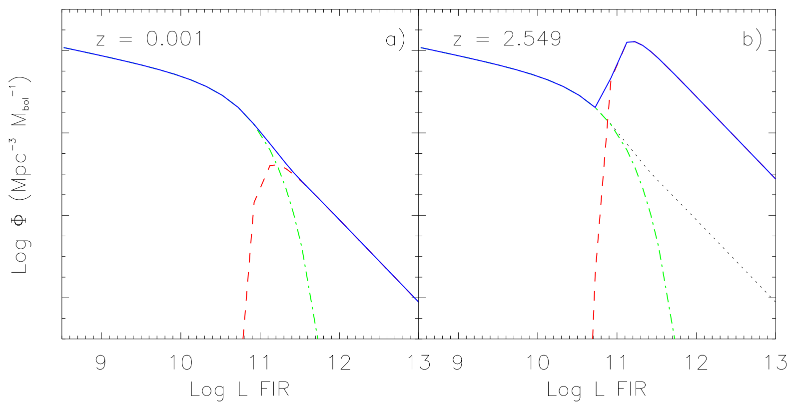

Fig. 3. a: Luminosity Function at z=0 (solid line); normal galaxy (dot-dash); ULIRG (dash-dash). b: Luminosity Function at z=2.5 (solid line); normal galaxy (dot-dash) ULIRG (dash-dash) and local LF (dots).

4.3 Model of Source Counts at 170 μm

The model at 170 μm, together with our data, is presented in Fig. 4. The brightest point of the observed counts is compatible with all our models, in particular the non-evolutionary scenario, which is expected for local sources. We also show the effect of the K-correction, which steepens the integral source count slope. Our evolutionary scenario fits the data within the error bars. Most of the background is expected to be resolved into sources once we are able to detect sources at the mJy level. This wavelength region, in which evolutionary effects are particularly important and where there are good prospects for detecting higher redshift sources because of the K-correction, is nowadays probably the best-suited range for probing galaxy evolution from space in the far-infrared.

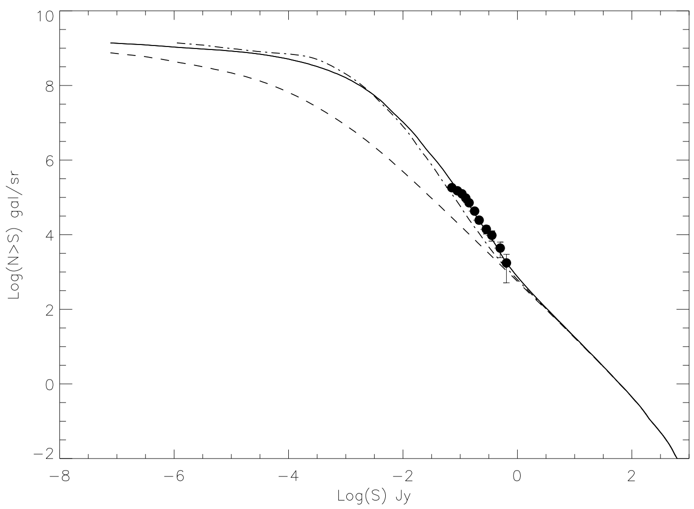

Fig. 4. Observed Counts and Models at 170 μm, with (solid line) and without (dashed line) evolution. The model with evolution and without K-correction is the dot-dash line.

4.4 Models of Source Counts at other wavelengths

Data at 15 μm [7], 90 μm [8] and 850 μm [2], with our models are presented in Fig. 5, Fig. 6 and Fig. 7 respectively.

At 15 μm, both the slopes and the little "waves" in the counts appear in the models with the combined effects of the K-correction and the evolution. At 90 μm, the K-correction does not emphasize the differences between the scenarii of evolution or non-evolution. At 850 μm, the "non smooth" appearance of our model is due to the discretization of the LF.

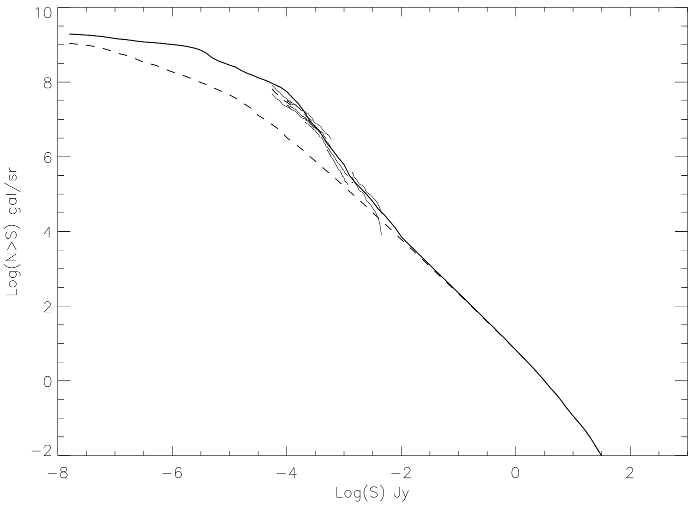

Fig. 5. Models at 15 μm with (solid line) and without (dashed line) evolution, and observed counts from Elbaz et al. [7] (thin lines).

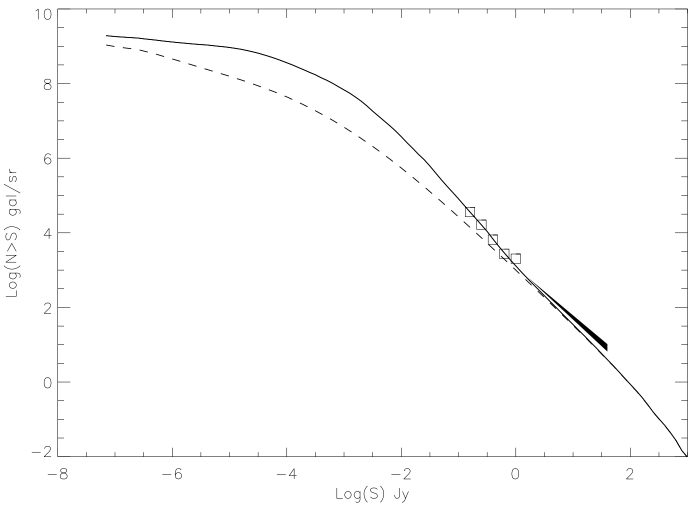

Fig. 6. Models at 90 μm with (solid line) and without (dashed line) evolution, and observed counts from Efstathiou et al. [8] (squares) and IRAS counts [8] (solid area)

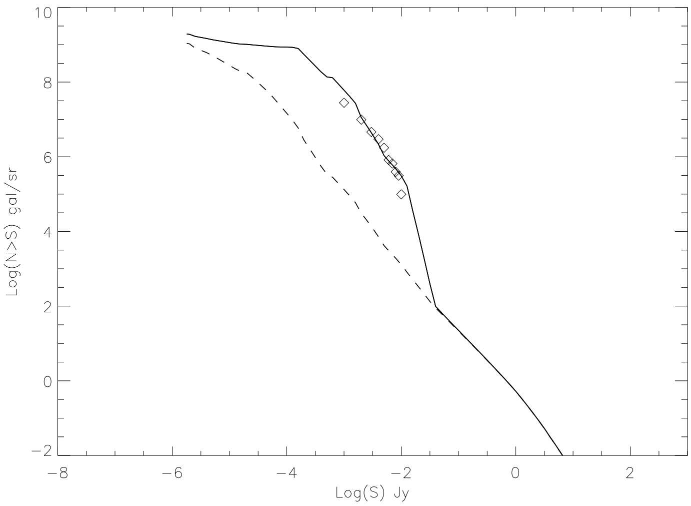

Fig. 7. Models at 850 μm with (solid line) and without (dashed line) evolution, and observed counts from Barger et al. [2] (diamonds).

5 Discussion

5.1 The bright end luminosity function evolution model

Our model of the evolving LF scenario fits most of the existing deep survey data from space (mid and far infrared) and ground (submillimetre). It is also compatible with the observational estimate of the LF in [17]. The strong observational constrain of multiwavelength source counts is thus explainable by a simple evolutionary law of the LF: the Bright End Luminosity Function Evolution (BELFE) model. One simple model is in agreement with all up-to-date observables and reproduces the background.

5.2 Redshift and Nature of the sources

Another crucial observational test for our model is the predicted vs observed redshift distribution. Although the statistics are poor, we have some evidence that most of the ISOCAM sources lie at redshift between 0 and 1.4 with a median at 0.8 [1], and that most of the SCUBA sources lie at redshifts greater than 2 [2]. Our predicted redshift distributions at these two wavelengths are in agreement with the existing observations.
What about FIRBACK 170 μm sources ? Our predicted redshift distribution shows that most of the sources lie at redshifts below 1.5, with a median comparable to that of the ISOCAM sources. This means that we are sensitive both to local sources and sources beyond redshift $z = 1$. All the FIRBACK sources with known redshifts (less than 10) [3], [22] are in this range. Two submillimetre sources are at $z > 1$, and a few visible sources are at $z \simeq 0.2$.

It is difficult to address the question differences between PHOT and CAM sources, because their redshift distributions (both expected and observed) are similar. About half of the 170 μm sources have 15 μm counterparts.

6 Conclusion

We have presented results from the FIRBACK survey, one of the largest ISO programs, dealing with resolved sources of the CIB: our source counts at 170 μm show strong evolution. This evolution is explained by a simple law involving the redshift of the luminosity function, which differs from pure density or luminosity evolution: the "Bright End Luminosity Function Evolution" model. The model fits all the existing source counts at 15, 90, 170 and 850 μm, and also predicts a redshift distribution in agreement with the (sometimes sparse) observations. This powerful tool, based on observational constraints on the CIB spectrum inversion and the local Luminosity Function, and on assumed template galaxy spectra, not only agrees with existing data but also is able to make useful predictions on source counts or CIB fluctuations. These predictions may be useful for planning the utilization of major telescopes of the future, such as SIRTF, Planck, FIRST and ALMA. All the FIRBACK materials are available at: `http://wwwfirback.ias.fr`.

References

1. Aussel, H., 1999, PHD Thesis Université Paris VII
2. Barger A.J., Cowie L.L., Sanders, D.B., 1999 ApJ, 518, L5
3. Dennefeld, M., 1999, Private Communication
4. Désert, F-X., Boulanger F., Puget, J.L., 1990, A&A, 237, 215
5. Dole H., Lagache G., Puget J-L., Gispert R., et al., 1999, ESA/SP-427, p1031, astro-ph/9902122
6. Dole H., Gispert R., Lagache G., Puget J-L., et al., 2000, in preparation
7. Elbaz D., et al., 1999, A&A, 351, L37
8. Efstathiou A., et al., 1999, MNRAS, submitted
9. Franceschini A., et al., 1998, MNRAS, 296, 709
10. Gispert R., Lagache G., Puget J-L., 2000, A&A, submitted
11. Guiderdoni B., et al., 1998, MNRAS, 295, 877
12. Kessler M. F., et al., 1996, A&A, 315, L27
13. Lagache G., and Puget J-L., 1999, A&A, in press, astro-ph/9910255
14. Lagache G., et al., 1999, this volume
15. Lagache G., and Dole, H., 2000, in preparation
16. Lemke D., et al., 1996, A&A, 315, L64
17. Lilly, Ss.J., et al, 1999, ApJ, 518, L641
18. Maffei B., 1994, PHD Thesis Université Paris-Sud
19. Puget J-L., et al., 1999, A&A, 345, 29
20. Puget J-L., et al., 1999, this volume
21. Sanders D.B., and Mirabel I.F., 1996, ARAA, 34, 749
22. Scott D., et al, 2000, A&A, in press, astro-ph/9910428
23. Soifer B.T., and Neugeubauer G., 1991, AJ, 101, 354
24. Tan J.C., Silk J., Balland C., 1999, ApJ, 522, 579